© 2018. Published by The Company of Biologists Ltd | Development (2018) 145, dev163956. doi:10.1242/dev.163956

RESEARCH ARTICLE

RhoA and ERK signalling regulate the expression of the transcription factor Nfix in myogenic cells

Valentina Taglietti[1,2], Giuseppe Angelini[1], Giada Mura[1], Chiara Bonfanti[1], Enrico Caruso[1], Stefania Monteverde[1], Gilles Le Carrou[3], Shahragim Tajbakhsh[3,4], Frédéric Relaix[2] and Graziella Messina[1,*]

ABSTRACT

The transcription factor Nfix belongs to the nuclear factor one family and has an essential role in prenatal skeletal muscle development, where it is a master regulator of the transition from embryonic to foetal myogenesis. Recently, Nfix was shown to be involved in adult muscle regeneration and in muscular dystrophies. Here, we have investigated the signalling that regulates Nfix expression, and show that JunB, a member of the AP-1 family, is an activator of Nfix, which then leads to foetal myogenesis. Moreover, we demonstrate that their expression is regulated through the RhoA/ROCK axis, which maintains embryonic myogenesis. Specifically, RhoA and ROCK repress ERK kinase activity, which promotes JunB and Nfix expression. Notably, the role of ERK in the activation of Nfix is conserved postnatally in satellite cells, which represent the canonical myogenic stem cells of adult muscle. As lack of Nfix in muscular dystrophies rescues the dystrophic phenotype, the identification of this pathway provides an opportunity to pharmacologically target Nfix in muscular dystrophies.

KEY WORDS: ERK kinases, Nfix, RhoA, Skeletal muscle, Signalling

INTRODUCTION

Nuclear factor one X (Nfix) belongs to the nuclear factor one (Nfi) family of transcription factors, which consists of four closely related genes in vertebrates: *Nfia*, *Nfib*, *Nfic* and *Nfix* (Gronostajski, 2000). We demonstrated previously that Nfix plays an essential role in prenatal skeletal muscle development, where it is responsible for the crucial checkpoint: the transcriptional switch from embryonic to foetal myogenesis (Messina et al., 2010; Pistocchi et al., 2013; Taglietti et al., 2016). Moreover, we reported that Nfix also regulates postnatal muscle homeostasis and the correct timing of muscle regeneration following injury (Rossi et al., 2016). Indeed, in the absence of Nfix, muscle regeneration is strongly delayed, indicating that Nfix is crucial for maintenance of the correct timing of skeletal muscle regeneration (Rossi et al., 2016).

Based on this evidence, we suggested that slower regenerating and twitching dystrophic musculature might be more protected from progression of the pathology through the silencing of *Nfix*, as in both α-sarcoglycan-deficient (*Sgca* null) (Duclos et al., 1998) and dystrophin-deficient (*mdx*) mice (Chapman et al., 1989). Indeed, lack of *Nfix* provides morphological and functional protection from degenerative processes through promotion of a more oxidative musculature and by slowing down muscle regeneration, which is in contrast to previous studies that were aimed at promoting of muscle regeneration (Rossi et al., 2017a). We thus provided the proof of principle to propose a new therapeutic approach to delay the progression of such pathologies that is based on slowing down the degeneration-regeneration cycle, instead of increasing the rate of regeneration. It is thus necessary to identify the molecular signalling pathways that regulates Nfix expression. Therefore, we focused on this signalling in the prenatal period, which is characterised by a defined temporal window of *Nfix* expression.

Prenatal skeletal muscle development is a biphasic process that involves differentiation of two distinct populations of muscle progenitors, known as the embryonic and foetal myoblasts (Biressi et al., 2007b; Hutcheson et al., 2009). In mouse, the process of embryonic myogenesis takes place around embryonic day (E) 10.5-12.5. During this phase, embryonic myoblasts are committed to differentiate into primary slow-twitch fibres, which establishes the primitive architecture of the prenatal muscles. Then, foetal myogenesis occurs between E14.5 and E17.5, when foetal myoblasts give rise to fast-twitching secondary fibres. This allows complete maturation of the prenatal muscles and confers fibre type diversification, which fulfil different functional demands of adult skeletal muscle (Schiaffino and Reggiani, 2011). *Nfix* expression is low during embryonic myogenesis and is strongly increased specifically during foetal myogenesis (Messina et al., 2010; Taglietti et al., 2016; Biressi et al., 2007b).

Embryonic and foetal myoblasts differ in terms of their morphology, extracellular signalling responses and gene expression profiles (Biressi et al., 2007a,b). These differences indicate that a transcriptional change is needed to switch from embryonic to foetal myogenesis. Nfix activates foetal-specific genes, such as muscle creatine kinase (*Ckm*) and β-enolase (*Eno3*), and represses embryonic-specific genes, such as *Myh7* (Messina et al., 2010; Taglietti et al., 2016), underscoring its crucial role as a regulator of this temporal switch.

To investigate the signalling that regulates *Nfix* expression, we examined JunB, the second most highly expressed transcription factor during foetal myogenesis (Biressi et al., 2007b). JunB is a member of the activator protein 1 (AP1) family, which is involved in maintenance of muscle mass and prevention of atrophy in adult muscles (Raffaello et al., 2010). However, the role of JunB during prenatal development is unknown. Here, we demonstrate that JunB is necessary for *Nfix* activation, which leads, in turn, to establishment of the foetal genetic programme. We also investigated the Rho GTPase RhoA because of its important roles in many intracellular signalling pathways (Amano et al., 1996; Kimura et al., 1996), which are mediated through activation of its major effector, the Rho-kinase ROCK. The interplay between the RhoA/ROCK pathway and various signalling molecules, such as the ERK kinases

[1]Department of Biosciences, University of Milan, 20133 Milan, Italy. [2]Biology of the Neuromuscular System, INSERM IMRB U955-E10, UPEC, ENVA, EFS, Creteil 94000, France. [3]Stem Cells and Development, Department of Developmental and Stem Cell Biology, Institut Pasteur, Paris 75015 France. [4]CNRS UMR 3738, Institut Pasteur, Paris 75015 France.

*Author for correspondence (graziella.messina@unimi.it)

V.T., 0000-0001-7166-6748; G.M., 0000-0001-8189-0727

Received 29 January 2018; Accepted 18 September 2018

Development (2018) 145, dev163956. doi:10.1242/dev.163956

(Zuckerbraun et al., 2003; Li et al., 2013), is known to promote the correct transduction of extracellular signals, and thus to condition the gene expression networks. Here, we report that the RhoA/ROCK axis defines the identity of embryonic myoblasts through repression of the activation of the ERK kinases and, as a consequence, of *JunB* and *Nfix*. Conversely, during foetal myogenesis, ERK activity is necessary for expression of JunB, which activates *Nfix*, to promote the beginning of the foetal myogenesis programme, and hence complete the maturation of prenatal muscle. Of particular interest, ERK activity is also necessary for *Nfix* expression in juvenile satellite cell-derived myoblasts, demonstrating that the ERK pathway is conserved from prenatal to postnatal myogenesis.

RESULTS

JunB regulates the expression of Nfix, which is then self-maintained

Although it has been demonstrated that *Nfix* and *JunB* are expressed at high levels specifically during foetal myogenesis (Biressi et al., 2007b), the temporal aspects of their expression profiles have not been defined in detail. We first used fluorescence-activated cell sorting (FACS) to analyse the transcript levels of *Nfix* and *JunB* in freshly isolated purified myoblasts from *Myf5*$^{GFP\text{-}P/+}$ embryonic muscle (Kassar-Duchossoy et al., 2004) at E11.5, E12.5 and E13.5, and from foetal muscle at E14.5, E15.5, E16.5 and E17.5. Both *Nfix* and *JunB* started to be expressed around E14.5, and their expression then increased at E15.5, remaining high up to E17.5 (Fig. S1A,B). Western blotting of total skeletal muscle lysates at these different stages showed similar profiles of Nfix and JunB expression, as also revealed by qRT-PCR (Fig. 1A, Fig. S1C,D). These data confirmed that *Nfix* and *JunB* expression occurs only during the foetal stages of muscle development, specifically from E14.5.

To better characterise the patterns of expression of Nfix and JunB in foetal muscle progenitors, we carried out immunostaining on *Myf5*$^{GFP\text{-}P/+}$-purified myoblasts obtained from foetuses at E14.5, E15.5 and E16.5. Freshly isolated myoblasts were maintained in culture for 2 h, to allow their adhesion, and then Nfix and JunB expression was monitored (Fig. 1B-C, Fig. S1E-F). At all time points analysed, a large proportion of the foetal myoblasts co-expressed Nfix and JunB (E14.5, 77.2%±2.52%; E15.5, 85%±4.14%; E16.5, 82%±3.91%), and at E14.5 and E15.5 there were some myoblasts positive for only JunB (E14.5, 10.3%±0.65%; E15.5, 10.2%±1.02%). Conversely, at E16.5, some myoblasts were positive for Nfix but not for JunB (13.9%±1.79%), and the

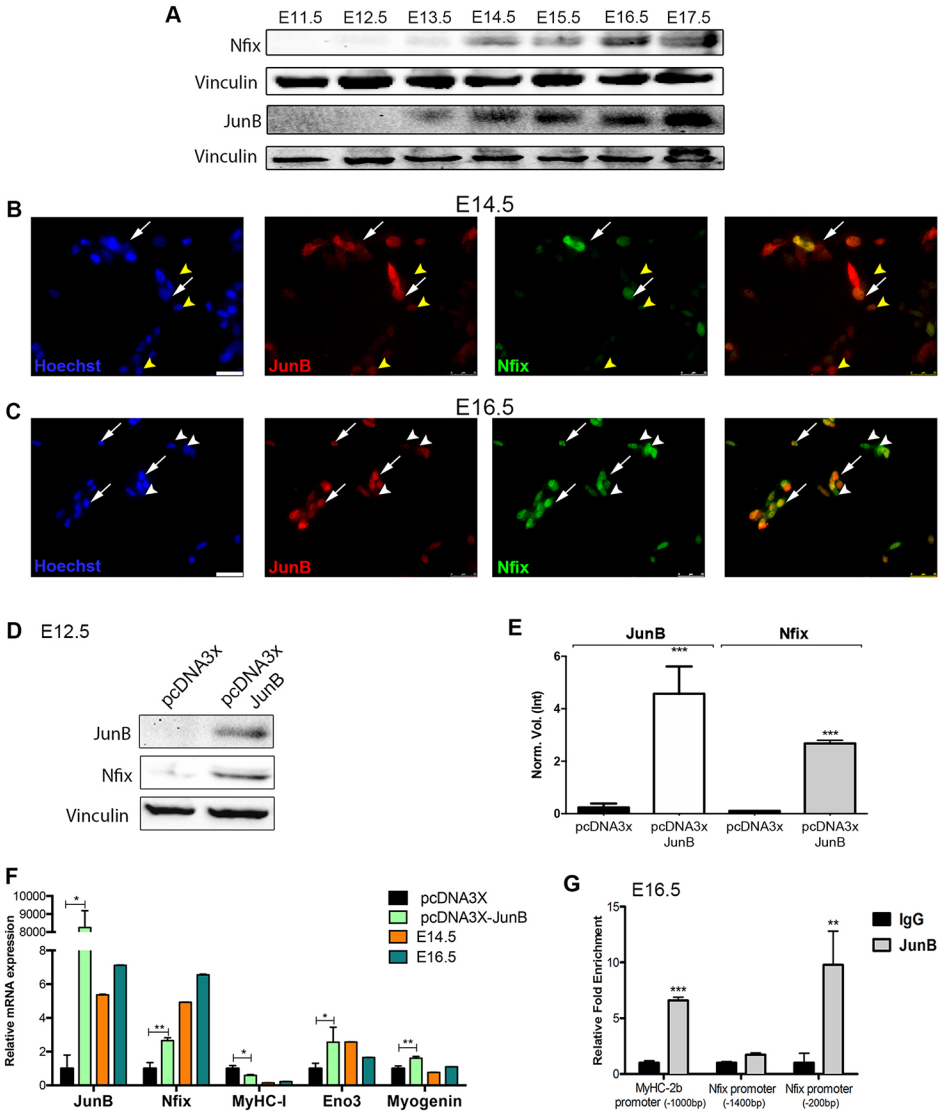

Fig. 1. Developmental timing of Nfix and JunB, and direct activation of Nfix.
(A) Representative western blots for Nfix and JunB for purified Myf5$^{GFP\text{-}P/+}$ myoblasts isolated from E11.5 to E17.5 muscle. Vinculin was used to normalise the total amount of loaded protein (JunB and Nfix were analysed on two separate gels, with data normalised to the respective vinculin). (B,C) Representative immunofluorescence for JunB (red) and Nfix (green) with freshly isolated Myf5$^{GFP\text{-}P/+}$-purified myoblasts at E14.5 (B) and E16.5 (C). Nuclei were counterstained with Hoechst. White arrows, myoblasts co-expressing JunB and Nfix; yellow arrowheads in B, nuclei positive for JunB and negative for Nfix; white arrowheads in C, myoblasts positive for Nfix but not for JunB. Scale bars: 25 µm. (D) Representative western blots of lysates from embryonic (E12.5) myoblasts overexpressing JunB (pcDNA3.1x-JunB) compared with control myoblasts (pcDNA3.1x). Vinculin was used to normalise the total amount of loaded protein. (E) Quantitative densitometry of Nfix and JunB in independent western blot experiments (***P<0.001; n=5). (F) qRT-PCR from Myf5$^{GFP\text{-}P/+}$-purified embryonic myoblasts (E12.5) transfected with the pcDNA3x-JunB overexpressing vector or with pcDNA3x. The data are compared with the endogenous levels at E14.5 and E16.5 muscles (*P<0.05; **P<0.01; n=5). (G) ChIP assay with anti-JunB antibodies for foetal myotubes (E16.5) on the positive control region (MyHC-2B promoter), the distal Nfix promoter region (1400 bp upstream of Nfix transcription start site) and the proximal Nfix promoter (−200 bp upstream of Nfix transcription start site). IgG was used as the unrelated antibody (**P<0.01; ***P<0.001; n=5).

Development (2018) 145, dev163956. doi:10.1242/dev.163956

increased number of Nfix-positive myoblasts at E16.5 is statistically significant compared with E14.5 (Fig. S1G).

As JunB appeared to be expressed earlier than Nfix, the interplay between Nfix and JunB was investigated. Embryonic myoblasts were transfected with the pcDNA3.1x-JunB expressing vector and the expression of Nfix then analysed by western blotting. Nfix was activated earlier in the embryonic myoblasts overexpressing JunB, compared with those with the only control vector (Fig. 1D,E). To further support this observation, *Myf5*$^{GFP\text{-}P/+}$-purified embryonic myoblasts were induced to express JunB upon pcDNA3.1x-JunB transfection, and the transcript levels of *Nfix* were examined by qRT-PCR. The population of embryonic myoblasts expressing JunB also expressed Nfix, whereas Nfix was essentially absent in the control myoblasts (Fig. 1F), suggesting that JunB was responsible for the activation of Nfix. As a consequence, JunB-positive embryonic myoblasts (and therefore Nfix) show earlier downregulation of the typical embryonic marker MyHC-I (Myh7) and upregulation of the foetal marker β-enolase. Indeed, Nfix has been shown to inhibit MyHC-I (Messina et al., 2010; Taglietti et al., 2016) and activate β-enolase (Messina et al., 2010). These data indicate that the induction of JunB in embryonic myoblasts promotes the expression of Nfix and, therefore, the activation of the foetal genetic programme.

To determine whether JunB can bind Nfix regulatory regions, *in silico* sequence analysis was performed for the *Nfix* promoter. The two AP-1 consensus sites [i.e. 5′-TGA(G/C)TCA-3′; Chinenov and Kerppola, 2001; Eferl and Wagner, 2003] were identified about 200 base pairs (bp) and 1400 bp upstream of the *Nfix* gene transcription start site. To determine whether JunB could bind these two sites, chromatin immunoprecipitation (ChIP) assays were carried out for JunB on differentiated foetal myoblasts (E16.5). As shown in Fig. 1G, JunB was directly bound to the *Nfix* promoter in the region that was proximal to the transcription start site (−200 bp), but not to the distal region (−1400 bp). The *MyHC-2b* promoter was used as the positive control sequence for the ChIP assays with JunB (Raffaello et al., 2010). Taken together, these data show that JunB therefore binds the Nfix promoter and, through an unknown mechanism, is able to regulate Nfix expression.

Similarly, we investigated whether the expression of Nfix in embryonic muscles can promote *JunB* expression in embryonic myoblasts transfected with the pCH-Nfix2 vector. However, the expression of *Nfix* did not induce *JunB* expression in the embryonic myoblasts (Fig. 2A). To support this observation, protein levels of JunB were determined in embryonic myoblasts purified from transgenic mice that overexpressed Nfix (i.e. *Tg:Mlc1f-Nfix2*) under the transcriptional control of the myosin light chain 1F promoter and enhancer (Jiang et al., 2002; Messina et al., 2010). JunB was essentially absent at E12.5 in the *Tg:Mlc1f-Nfix2* embryonic myoblasts, as in the wild-type littermates (Fig. 2B, Fig. S2A). As expected, JunB was also

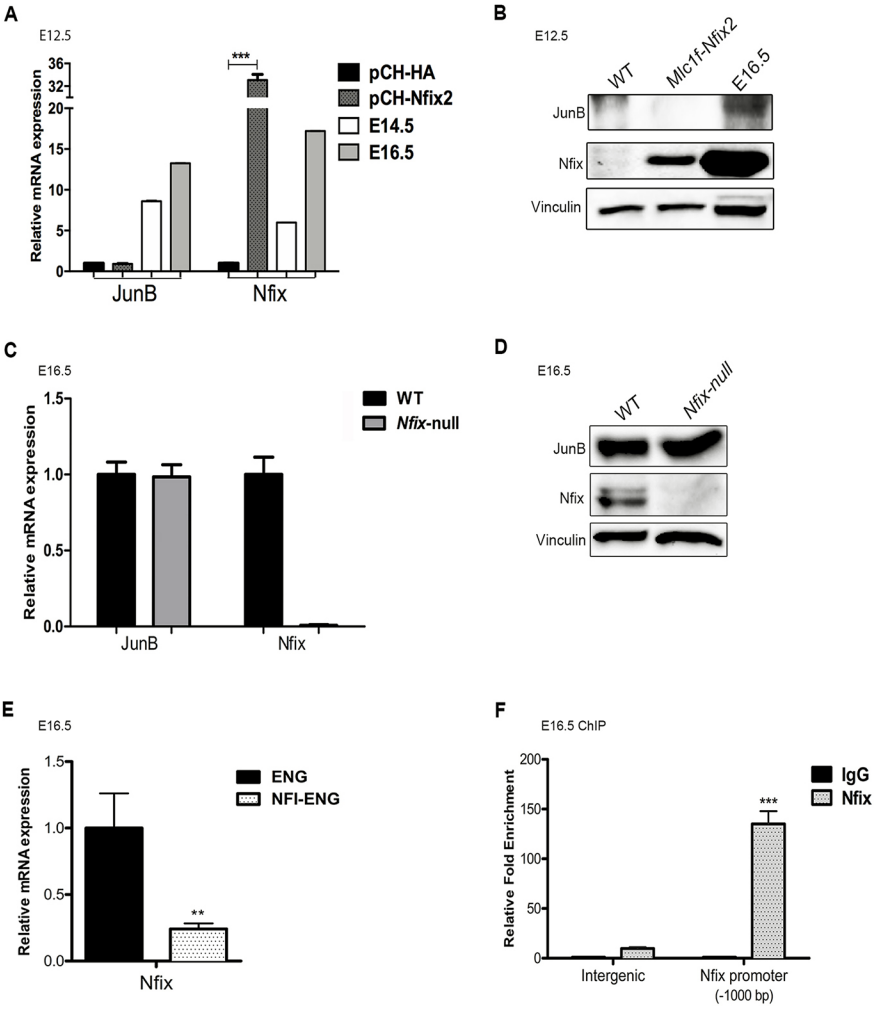

Fig. 2. Nfix does not regulate JunB, but promotes its own expression. (A) qRT-PCR for JunB and Nfix for embryonic (E12.5) myoblasts transfected with the Nfix-overexpressing vector (pCH-Nfix2) or the control vector (pCH-HA). The data are compared with the endogenous levels at E14.5 and E16.5 muscles (***P<0.01; n=5). (B) Representative western blots for Nfix and JunB of protein extracts from wild-type and Tg:*Mlc1f*-Nfix2 embryonic muscle (E12.5) with foetal muscle (E16.5) as positive control. Vinculin was used to normalise the total amount of loaded protein. (C) qRT-PCR for JunB and Nfix on wild-type and *Nfix*-null foetal muscle (E16.5). (D) Representative western blots for Nfix and JunB on lysates from wild-type and *Nfix*-null foetal muscle (E16.5). Vinculin was used to normalise the total amount of loaded protein. (E) qRT-PCR for Nfix on foetal myoblasts transfected with the dominant-negative NFI-engrailed (NFI-ENG) compared with foetal myoblasts expressing engrailed domain (ENG) (**P<0.01; n=5). (F) ChIP assay using anti-Nfix antibodies on foetal myotubes to test Nfix binding to its own promoter (−1000 bp; Nfix promoter). An intergenic region was used as the negative control and IgG as the unrelated antibody (***P<0.01).

Development (2018) 145, dev163956. doi:10.1242/dev.163956

expressed normally in *Nfix*-null foetal myoblasts (Campbell et al., 2008) (Fig. 2C-D, Fig. S2B), indicating that Nfix does not control *JunB* expression.

To determine whether once expressed, *Nfix* can maintain its own expression, foetal myoblasts were transduced with a lentiviral vector that expressed a dominant-negative Nfi-engrailed (NFI-ENG) fusion protein composed of the *Drosophila* ENG transcriptional repression domain fused with the Nfia DNA-binding and dimerisation domain (Bachurski et al., 2003). Overexpression of NFI-ENG resulted in inhibition of Nfi factor transactivation activity, as NFI-ENG acts as a dominant-negative form (Messina et al., 2010). The NFI-ENG foetal myoblasts showed strong downregulation of *Nfix* compared with the control foetal myoblasts that expressed only the engrailed domain (ENG) (Fig. 2E). This indicated that Nfi factors can activate the transcription of Nfix.

To further support these data, ChIP assays were carried out for Nfix in differentiated foetal myoblasts. These showed direct binding of Nfix to its own promoter at an NFI consensus binding site located 1000 bp upstream of the *Nfix* gene transcription start site (Fig. 2F). Taken together, these data demonstrate that Nfix, once activated by a mechanism that in part involves JunB, is able in turn to promote its own expression.

JunB is necessary for Nfix induction, but not for the direct activation of the foetal myogenic programme

As we showed that JunB promotes the expression of *Nfix* in embryonic myoblasts, we then investigated whether JunB is necessary to activate the myogenic foetal programme (Messina et al., 2010). For this reason, cell sorting was used to isolate foetal myoblasts from E16.5 $Myf5^{GFP\text{-}P/+}$ muscles, and JunB was silenced using a small-hairpin RNA (shJunB, foetal myoblasts). As control, $Myf5^{GFP\text{-}P/+}$-purified foetal myoblasts were transduced with a scrambled lentiviral vector that targeted a non-related sequence. When cultured under conditions that promote differentiation, the purified foetal myoblasts silenced for JunB showed the standard embryonic phenotype, which was characterised by mononucleated myocytes and multinucleated myotubes that contained only a few nuclei (Biressi et al., 2007b). This specific inhibition of JunB decreased the expression of Nfix (Fig. 3A,B), whereas the typical embryonic marker MyHC-I was greatly induced (Fig. 3C).

As the foetal programme was affected, we investigated whether in shJunB foetal myoblasts, the effects on foetal myogenesis were specifically due to the lack of JunB, or were the consequence of downregulation of Nfix. Purified shJunB foetal myoblasts were transduced with an HA-tagged *Nfix2* expression vector

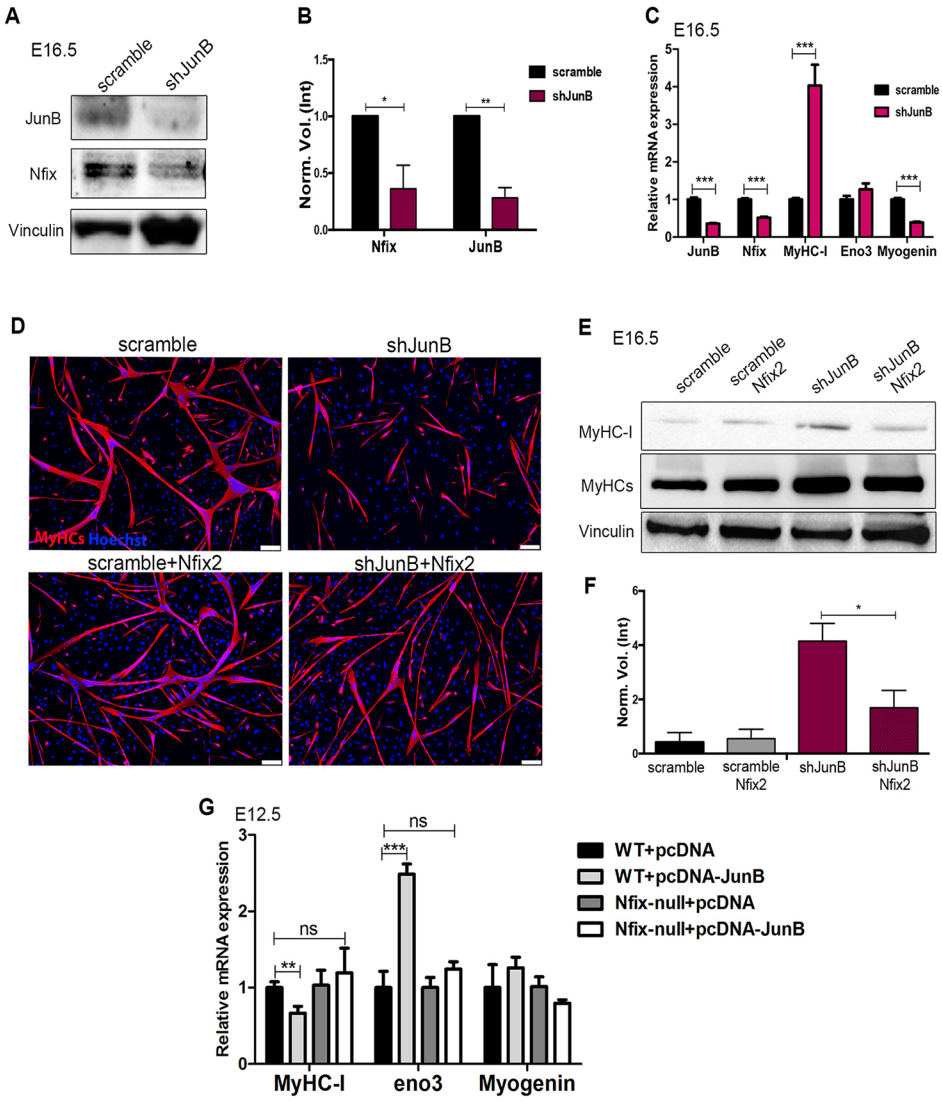

Fig. 3. Silencing of JunB leads to the acquisition of embryonic features as a consequence of downregulation of Nfix. (A) Representative western blots of shJunB and control (scramble) foetal differentiated myoblasts. Vinculin was used to normalise the total amount of loaded protein. (B) Quantitative densitometry of Nfix and JunB of five independent western blot assays (*P<0.05; **P<0.01; n=5). (C) qRT-PCR of $Myf5^{GFP\text{-}P/+}$-purified foetal myoblasts infected with lenti-shJunB or the scramble vector, for analysis of expression of Nfix and MyHC-I (***P<0.001). (D) Representative immunofluorescence images of differentiated $Myf5^{GFP\text{-}P/+}$-purified foetal myoblasts co-transduced with the shJunB and HA-Nfix2 lentivectors (shJunB+Nfix2) or the single and non-targeting (scramble) vectors as controls, showing MyHCs (MF20; red) and Hoechst (blue). Scale bars: 100 µm. (E) Representative western blots of differentiated foetal myoblasts (scamble+pCH-HA, scramble +Nfix2, shJunB+pCH-HA and shJunB+Nfix2) showing MyHC-I expression. MyHCs (MF20) and vinculin were used to normalise the total amount of loaded protein. (F) Densitometric quantification of MyHC-I protein versus vinculin (*P<0.05; n=5). (G) qRT-PCR of wild-type and *Nfix*-null embryonic myoblasts transfected with the JunB-overexpressing vector or with the control vector (pcDNA) (**P<0.01; ***P<0.001; n=5).

Development (2018) 145, dev163956. doi:10.1242/dev.163956

(shJunB+Nfix2) (Fig. S2C) and cultured under differentiating conditions. After 3 days *in vitro*, silencing of JunB reduced the number of nuclei per myotube (Fig. S2D), the fusion index (Fig. S2E) and the area of each myotube (Fig. S2F), which indicated impaired foetal myoblast differentiation and fusion. More importantly, the foetal shJunB+Nfix2 cultures contained larger myotubes than the foetal shJunB cultures, with more nuclei in clusters in the centres of the myotubes (Fig. 3D). Furthermore, the morphology of the shJunB+Nfix2 myotubes was similar to those for both scrambled and Nfix2-transduced cultures, showing a significant rescue of the analysed morphological parameters (Fig. 3D, Fig. S2D-F), which indicated that the rescue of Nfix function in shJunB foetal myoblasts was sufficient to reactivate the foetal programme. To determine whether this rescue was associated with a phenotypic change, western blotting was used to examine the expression of the typical embryonic marker MyHC-I. As shown in Fig. 3E,F, the shJunB foetal myoblasts expressed high levels of slow MyHC-I after differentiation, whereas this upregulation of MyHC-I was not seen for the differentiated shJunB+Nfix2 foetal myoblasts, with downregulation of MyHC-I seen instead, as expected. Moreover, wild-type embryonic myoblasts overexpressing JunB showed downregulated MyHC-I and activated β-enolase as a consequence of the Nfix upregulation. In contrast, in the *Nfix*-null embryonic myoblasts, overexpression of JunB did not lead to any changes in MyHC-I and β-enolase, as the markers of embryonic and foetal myogenesis, respectively (Fig. 3G, Fig. S2G). These data demonstrate that, although JunB is required for *Nfix* induction, it is not sufficient to activate the foetal myogenic programme. Hence, Nfix acts downstream of JunB and is strictly required for activation of the foetal myogenic programme.

The RhoA/ROCK axis negatively regulates ERK activity

We next aimed to identify the upstream signalling necessary for *JunB* induction, and therefore for *Nfix* expression. The Rho GTPase RhoA is required for the myogenic process, and its activity must be finely regulated in time for correct muscle differentiation (Castellani et al., 2006). To determine whether RhoA activity is regulated temporally during prenatal muscle development, GST-Rhotekin pull-down assays were performed on lysates of E12.5, E14.5 and E16.5 myoblasts, with active Rho GTPases quantified by western blotting. As shown in Fig. 4A, GTP-bound activated Rho was increased at E12.5 and E14.5, whereas at E16.5 it decreased. Thus, the Rho GTPases were selectively activated during embryonic myogenesis and shut down at the foetal stage. Five independent pull-down experiments were quantified through the normalisation of the relative amount of pixel intensity (Int) on the reference band, showing a statistically significant decrease in RhoA activity at E16.5 compared with both E12.5 and E14.5 (Fig. S2H).

RhoA is an upstream activator of ROCK kinases and requires ROCK activity for its effects, which also impinge upon myogenesis (Nishiyama et al., 2004; Pelosi et al., 2007). Thus, to support the activation of RhoA signalling during embryonic myogenesis, phosphorylation of the specific ROCK substrate MYPT1 on Thr 696 was examined during prenatal skeletal muscle development (Seko et al., 2003; Murányi et al., 2005). As shown in Fig. 4B and quantified in Fig. S3A, MYPT1 phosphorylation was seen only during the early phase of myogenesis, between E11.5 and E12.5, which confirmed that RhoA and ROCK are both active during primary myogenesis.

The RhoA/ROCK axis is known to regulate the signalling of many intracellular substrates, such as the ERK kinases (Zuckerbraun et al., 2003; Li et al., 2013). The activities of the ERK kinases were therefore examined during prenatal development, as determined by their phosphorylation. Indeed, the phosphorylated ERKs were seen only during foetal myogenesis, from E14.5 to E17.5 (Fig. 4C, Fig. S3B). Given that RhoA/ROCK signalling might be involved in embryonic to foetal transition, embryonic myoblasts were treated with the ROCK inhibitor Y27632 (Uehata et al., 1997). Proliferation, differentiation and apoptosis were assessed after 3 days of Y27632 or vehicle treatment (Fig. 4D-I). EdU incorporation, after a single 2 h pulse, and the apoptosis (quantification of embryonic myoblasts expressing the cleaved and active form of caspase 3) did not show significant changes between Y27632-treated and control cells (Fig. 4D-F). Conversely, the morphology of Y27632-exposed embryonic myotubes resembled the typical feature of foetal differentiated fibres with a tendency for increased fusion index (Fig. 4G-I), suggesting a precocious switch toward the foetal phase. To better elucidate the changes induced by ROCK inhibition, we evaluated ERK activity by immunoblotting and showed that embryonic myoblasts treated with Y27632 had greatly increased ERK activity (Fig. 4J). Conversely, activated phospho-ERK (pERK) decreased in foetal myoblasts expressing the activated RhoA (RhoV14), compared with control cells (Fig. 4J). Densitometric quantification of embryonic myoblasts treated with Y27632 or vehicle and of foetal myoblasts expressing RhoV14 or a control plasmid revealed a significant increase of pERK in embryonic cells treated with ROCK inhibitor, expressed as a ratio of the total amount of ERK kinases. In contrast, foetal myoblasts expressing RHOV14 showed a statistically significant decrease in the content of activated ERK (Fig. 4K). Taken together, these data indicate that ROCK mediates the negative regulation that RhoA signalling has on ERK kinase activity.

The ERK kinases are modulated upon RhoA/ROCK misregulation in muscle progenitors

To determine whether the RhoA/ROCK axis has a role in regulation of JunB and Nfix, the effects of the ROCK inhibitor Y27632 on $Myf5^{GFP\text{-}P/+}$-purified embryonic myoblasts were analysed. Here, ROCK inhibition led to increased *Junb* and *Nfix* expression, but did not affect myogenin and MyHC-emb expression (Fig. 5A). As expected, genes specifically expressed during embryonic myogenesis, such as *Myh7*, *Smad6* and *Tcf15* (Biressi et al., 2007a,b), were decreased and an earlier expression of a panel of foetal genes, such as β-enolase (*Eno3*), *Nfia*, *Ckm* and *Prkcq* was observed (Figs 5A, S3C).

The effects of ROCK inhibition on the early expression of *Junb* and *Nfix* and on the downregulation of slow MyHC were also investigated by western blotting (Fig. 5B), and quantified in Fig. S3D. $Myf5^{GFP\text{-}P/+}$-purified foetal myoblasts that were transduced with a lentiviral vector expressing the constitutively active form of RhoA (RHOV14) showed a dramatic decrease in JunB and Nfix mRNA levels. Instead, MyHC-I was highly expressed, rather than being repressed, which indicated that RHOV14-expressing foetal myoblasts acquired a more embryonic-like gene transcription profile (Fig. 5C). Western blotting confirmed that the JunB and Nfix foetal transcription factors were downregulated in the RHOV14 foetal myoblasts, whereas MyHC-I was significantly induced (Fig. 5D and Fig. S3E).

As the RhoA and ROCK axis is able to block the activation of ERK (Li et al., 2013), we hypothesised that the ERK kinases might regulate *Junb* and *Nfix* expression. Thus, foetal myoblasts were treated with the ERK antagonist PD98059, which selectively inhibits MEK kinases, preventing the activation of ERK signalling. First, we analysed the effects of ERK inhibition on foetal myoblasts

Development (2018) 145, dev163956. doi:10.1242/dev.163956

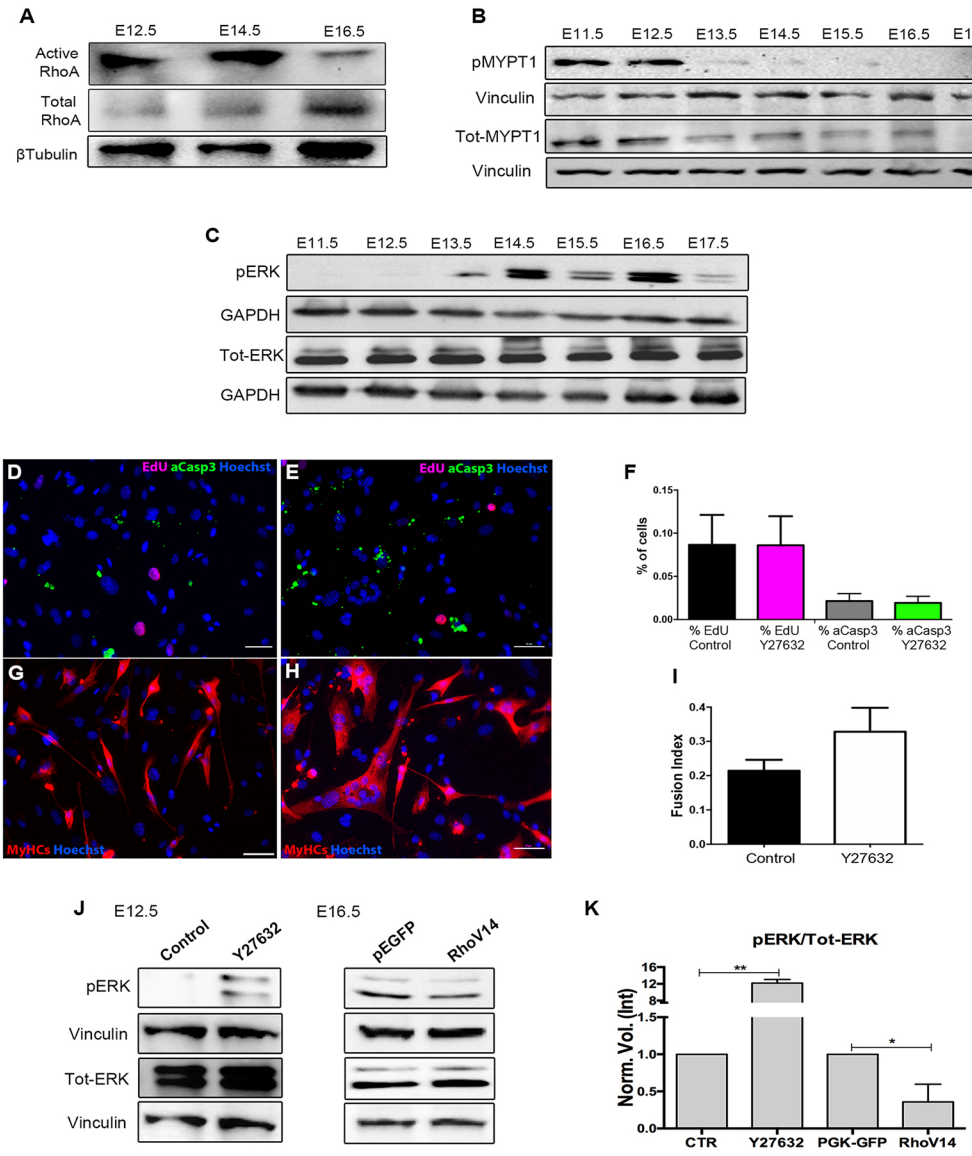

Fig. 4. The RhoA/ROCK axis inhibits ERK kinase activity during embryonic myogenesis. (A) Representative pull-down assay of lysates of myoblasts at E12.5, E14.5 and E16.5. Active Rho GTPases were detected using western blotting, and the amount of input is shown in the lower panel (total RhoA). β-Tubulin was used to normalise the total input. (B,C) Representative western blots of E11.5 to E17.5 muscle for MYPT1 phosphorylated at Thr696 by ROCK (B) and for phosphorylated ERK (pERK) and total ERK (Tot-ERK) (C). In B, total MYPT1 (Tot-MYPT1) and vinculin were used to normalise the loaded protein; to avoid cross-reactions between the antibodies, the same samples were analysed on separate gels. In C, GAPDH was used to normalise the loaded protein, and although the antibodies against tot-ERK and pERK were raised in different species, the same samples were analysed on separate gels. (D,E) Immunofluorescence for cleaved caspase 3 (active caspase, aCasp3) and EdU detection on embryonic (E12.5) myotubes treated with vehicle (D) or Y27632 (E) for 3 days until the differentiation. (F) Quantification of the percentage of cells positive for EdU, upon 2 h EdU pulse, and of the percentage of cells expressing cleaved caspase 3 (aCasp3) at the nuclear and/or perinuclear level. The quantification was performed on differentiated embryonic myotubes after the daily treatment with Y27632. No significant changes were observed between control and Y27632-treated cells (n=5). (G,H) Immunofluorescence for sarcomeric myosins (MyHCs) and Hoechst of control (G) and Y27632-treated (H) embryonic myotubes. (I) Graph illustrating the fusion index, calculated as ratio of nuclei number in myocytes/myotubes on the total number of nuclei (n=5). (J) Representative western blots of: embryonic myoblasts (E12.5) treated with the ROCK inhibitor Y27632 or with vehicle (left); and foetal myoblasts (E16.5) transduced with the lentivirus expressing constitutively activated RhoA (RHOV14) or the control (PGK-GFP) (right). Vinculin was used to normalise the amount of loaded protein. (K) Quantitative densitometry of phosphorylated (p)ERK normalised according to the ratio between total ERK and vinculin (*P<0.05; **P<0.01; n=5).

by examining proliferation, apoptosis, differentiation and the fusion index. Both proliferation, after an EdU pulse of 2 h, and apoptosis were not affected by ERK inhibition (Fig. 5E-G), whereas only incubation for 12 h with PD98059 delayed the differentiation of foetal myoblasts, as demonstrated by the decrease of the fusion index compared with the control cells (Fig. 5H-J), and changed the expression of some genes specifically expressed during embryonic or foetal myogenesis (Fig. S3F).

Western blot was used to examine JunB and Nfix protein levels. The immunoblot in Fig. 5K and the densitometric analysis in Fig. S3G show that expression of JunB and Nfix was indeed reduced in these PD98059-treated foetal myoblasts. These results indicate that activation of ERK kinases can promote foetal myogenesis through the activation of JunB and Nfix.

We then examined whether the ERKs are the RhoA/ROCK signalling downstream targets during myogenesis. As shown

Development (2018) 145, dev163956. doi:10.1242/dev.163956

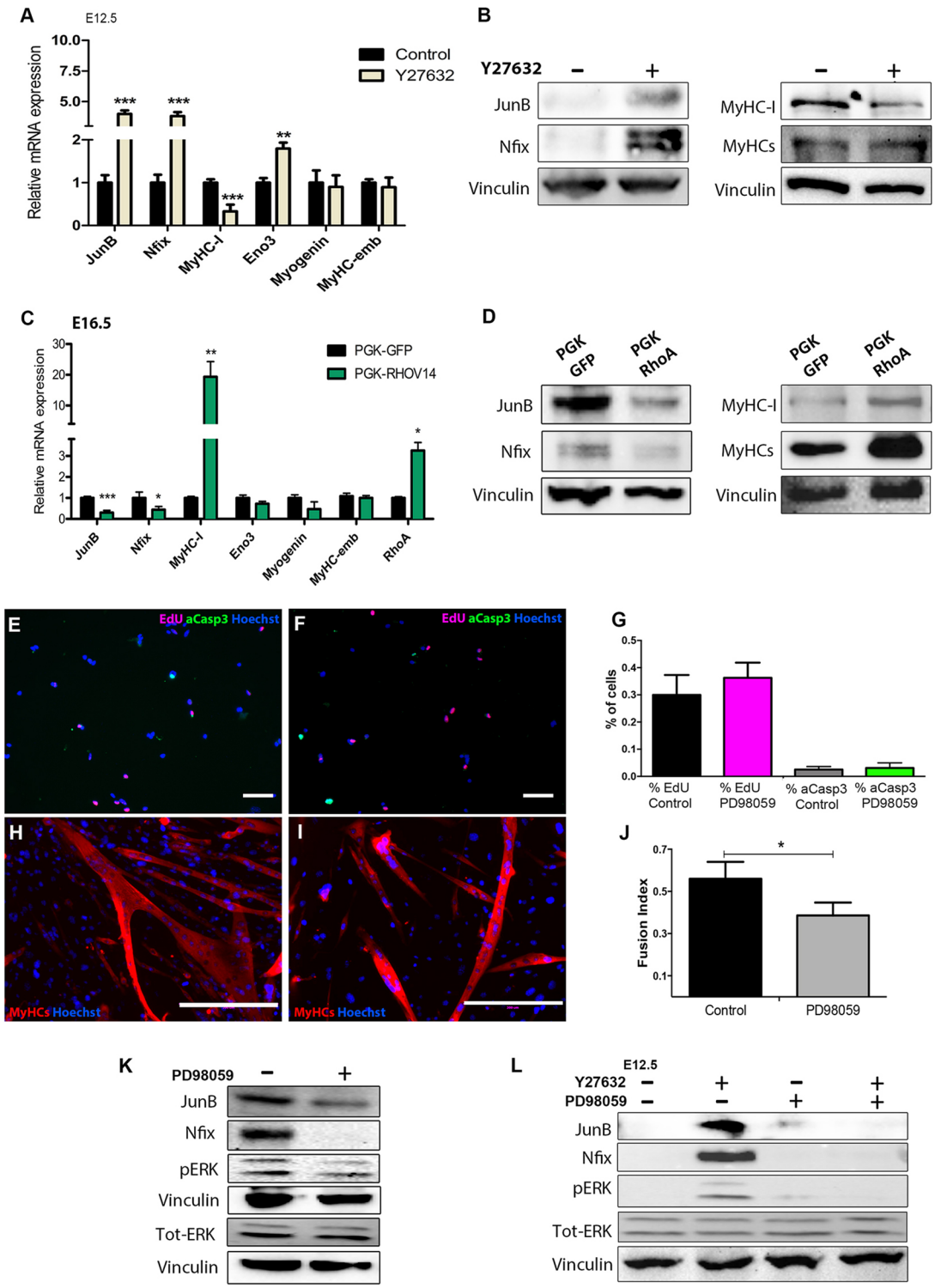

Fig. 5. RhoA and ROCK activities inhibit foetal myogenesis through inhibition of JunB and Nfix, while ERK activity promotes JunB and Nfix expression. (A) qRT-PCR for expression of embryonic and foetal markers of Myf5$^{GFP\text{-}P/+}$-purified embryonic myoblasts treated with the ROCK inhibitor Y2763 or vehicle (**P<0.01; ***P<0.001; n=5).(B) Representative western blot of embryonic myoblasts treated with the ROCK inhibitor Y2763 or not treated. MyHCs (MF20) and vinculin were used to normalise the total amount of loaded protein. (C) qRT-PCR for expression of embryonic and foetal markers of Myf5$^{GFP\text{-}P/+}$-purified foetal myoblasts transduced with constitutively activated RhoA (PGK-RhoV14) or control (PGK-GFP) lentivectors (*P<0.05; **P<0.01). (D) Representative western blots for JunB, Nfix and MyHC-I of foetal myoblasts overexpressing constitutively activated RhoA (PGK-RHOV14) or control (PGK-GFP). MyHCs (MF20) and vinculin were used to normalise the total amount of loaded protein. (E,F) EdU detection and immunofluorescence for active and cleaved caspase 3 (aCasp3) on control (E) and PD98059-treated (F) foetal myoblasts (n=5). (G) Quantification of the percentage of EdU- or aCasp3-positive cells (n=5). (H,I) Immunofluorescence for sarcomeric myosins (MyHCs) and Hoechst of control (H) and PD98059-treated (I) foetal myotubes. (J) Graph illustrating the fusion index of foetal myotubes treated with vehicle only (control) or with the ERK inhibitor PD98059 (*P<0.05; n=5). (K) Representative western blots of foetal myoblasts treated with the ERK inhibitor PD98059 or vehicle. Vinculin was used to normalise the total amount of loaded protein. (L) Representative western blots of embryonic myoblasts treated with the ROCK inhibitor Y27632 and/or the ERK inhibitor PD98059 or vehicle.

Development (2018) 145, dev163956. doi:10.1242/dev.163956

in Fig. 5L and in Fig. S3H-J, ROCK inhibition in embryonic myoblasts enhanced ERK phosphorylation and activation, which led to upregulation of JunB and Nfix. Furthermore, treatment with Y27632 (ROCK inhibitor) and PD98059 (ERK antagonist) led to reductions in JunB and Nfix expression, as in the control embryonic myoblasts. These data indicate that the ERK kinases are downstream effectors of RhoA/ROCK during prenatal myogenesis, and that ERK activity is necessary for activation of JunB and Nfix.

ERK kinases regulate Nfix expression *in vivo*

To determine whether ERK inhibition can also modify Nfix regulation *in vivo*, foetuses were exposed to PD98059. Pregnant mice were treated on day 15.5 of gestation (E15.5) with a single systemic injection of either vehicle (dimethylsulfoxide) or 10 mg/kg PD98059, and the foetuses were harvested the day after (Fig. 6A). Western blotting of myoblasts isolated from these foetuses demonstrated that PD98059 treatment decreased the phosphorylation of the ERK kinases (pERK), which was associated with downregulation of Nfix and of JunB (Fig. 6B). The reduction of Nfix, JunB and pERK protein levels were also measured by densitometric quantification (Fig. 6C). Morphologically, the PD98059-exposed foetal muscles showed a shift in myofibre area distribution towards smaller values compared with the control (Fig. 6D-F), which correlates with the reduction in the fusion index observed *in vitro* (Fig. 5H-J).

Furthermore, immunofluorescence analysis of foetal cross-sections with antibodies directed against all of the sarcomeric myosins and Nfix (Fig. 6G-L) clearly showed a reduction of Nfix in foetal muscle. Consistent with this observation, we noted a significant decrease in the percentage of myonuclei expressing Nfix upon PD9589 treatment compared with the control (Fig. 6O). In addition, Nfix expression was not altered in the extra-muscular tissues of these PD98059-exposed foetuses, which indicated that the ERK kinases regulate Nfix specifically in developing skeletal muscle. To validate the finding that the downregulation of Nfix specifically occurred in myogenic foetal progenitors, we performed immunofluorescence for Pax7, a marker of the myogenic lineage, and Nfix on muscle sections of control and PD98059-exposed foetuses. As shown in Fig. 6M,N and quantified in Fig. 6P, upon PD98059 treatment, there was a lower number of cells co-expressing Pax7 and Nfix, indicating that systemic injection of PD98059 suppresses Nfix expression in foetal muscle *in vivo*.

ERK kinases also control Nfix postnatally

Recently, we demonstrated that Nfix is expressed also in adult muscle satellite (stem) cells (Rossi et al., 2016), and that its

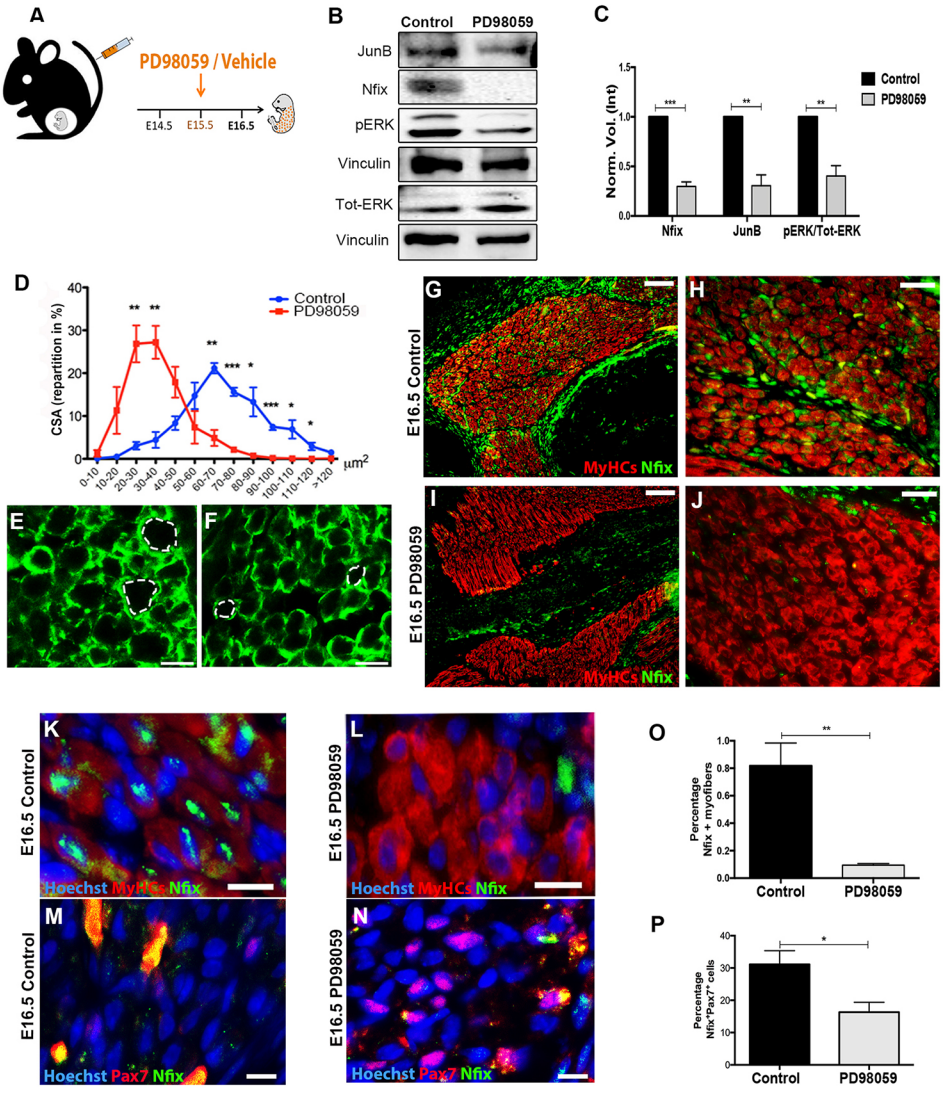

Fig. 6. Inhibition of ERK activity blocks Nfix expression *in vivo*. (A) Experimental scheme of PD98059 administration to pregnant mice at E15.5. (B) Representative western blots of foetal myoblasts isolated from PD98059-treated or control (vehicle) foetuses. Vinculin was used to normalise the total amount of loaded protein. (C) Quantitative densitometry of Nfix, JunB and the ratio of pERK to total ERK. (**P<0.01; ***P<0.001; n=5). (D) Myofibre cross-sectional area (CSA) distribution in foetal muscles treated with vehicle only or PD98059 (*P<0.05; **P<0.01; ***P<0.001; n=5). (E,F) Representative immunofluorescence images of control (E) or PD98059-treated (F) foetal muscles using anti-laminin antibody. The dotted lines highlight the CSA of the foetal fibres. Scale bars: 25 µm. (G-J) Representative immunofluorescence images of muscle sections from E16.5 control (G,H) and PD98059-treated (I,J) foetuses using anti-MyHCs (red) and Nfix (green) antibodies. Scale bars: 50 µm, in G,I; 25 µm in H,J. (K,L) High magnification of the immunofluorescence on control and PD98059-exposed foetal muscle sections with anti-MyHCs (red) and Nfix (green) antibodies. Scale bars: 10 µm. (M,N) High magnification of the immunofluorescence on control and PD98059-exposed foetal muscle sections with Pax7 (red) and Nfix (green) antibodies. Scale bars: 10 µm. (O) Quantification of the percentage of Nfix-positive myonuclei in foetuses treated with PD98059 or vehicle (**P<0.01; n=5). (P) Quantification of the percentage of Pax7-positive cells expressing Nfix in PD98059-treated or control foetuses (*P<0.05; n=5).

Development (2018) 145, dev163956. doi:10.1242/dev.163956

silencing appears to be a promising approach to ameliorate dystrophic phenotypes and to slow down the progression of these pathologies (Rossi et al., 2017b). To determine whether RhoA/ROCK-ERK signalling is also involved in Nfix regulation in skeletal muscle stem cells (MuSCs), we first characterised the timing of RhoA/ROCK and ERK expression and activation in juvenile MuSC-derived myoblasts, isolated at postnatal day 10 (P10), from their proliferation to 4 days in differentiation media (dDM). Western blotting revealed transient activation of the ERK kinases (Fig. 7A and Fig. S4A, pERK) during proliferation and in the early phase of differentiation (1dDM). Conversely, ROCK kinase was specifically active during the later phases of differentiation, as seen by specific phosphorylation of the ROCK substrate (Fig. 7A and Fig. S4B, pMyPT1). However, JunB was specifically expressed only during the proliferation phase (Fig. S4C), whereas Nfix showed higher expression at 1dDM, but its expression was maintained throughout differentiation (Fig. 7A and Fig. S4D), when there was little or no ERK activity.

We then asked whether this ERK-independent expression of *Nfix* in the later phases of differentiation is due to Nfix-mediated activation of its own expression. Juvenile MuSCs (P10) were transduced with lentiviral vectors that expressed dominant-negative Nfi-engrailed (NFI-ENG) or the control (ENG), and the cells were differentiated for 3 and 4 days (i.e. 3dDM, 4dDM). As shown in Fig. S4E,F, expression of NFI-ENG was associated with decreased expression of Nfix, which indicated that Nfix was necessary for maintaining its own expression.

To determine whether the ERK and RhoA/ROCK pathways are also conserved in the regulation of *Nfix* expression in postnatal myogenesis, RhoA/ROCK and ERK activities were inhibited in MuSCs. Isolated juvenile MuSC-derived myoblasts were treated during proliferation with PD98059, to inhibit ERK signalling in the phase of its highest activation, whereas they were exposed to a ROCK inhibitor, Y27632, during differentiation (2dDM), when the ROCK kinases are active.

First, we tested the effect of PD98059 and Y27632 on MuSC behaviour, analysing by western blot the expression of Pax7, myogenin and sarcomeric myosins after the differentiation (2dDM) (Fig. S4G-H) or during the proliferation phase (PD98059 treatment, Fig. S4J,K); we did not observe any significant difference between

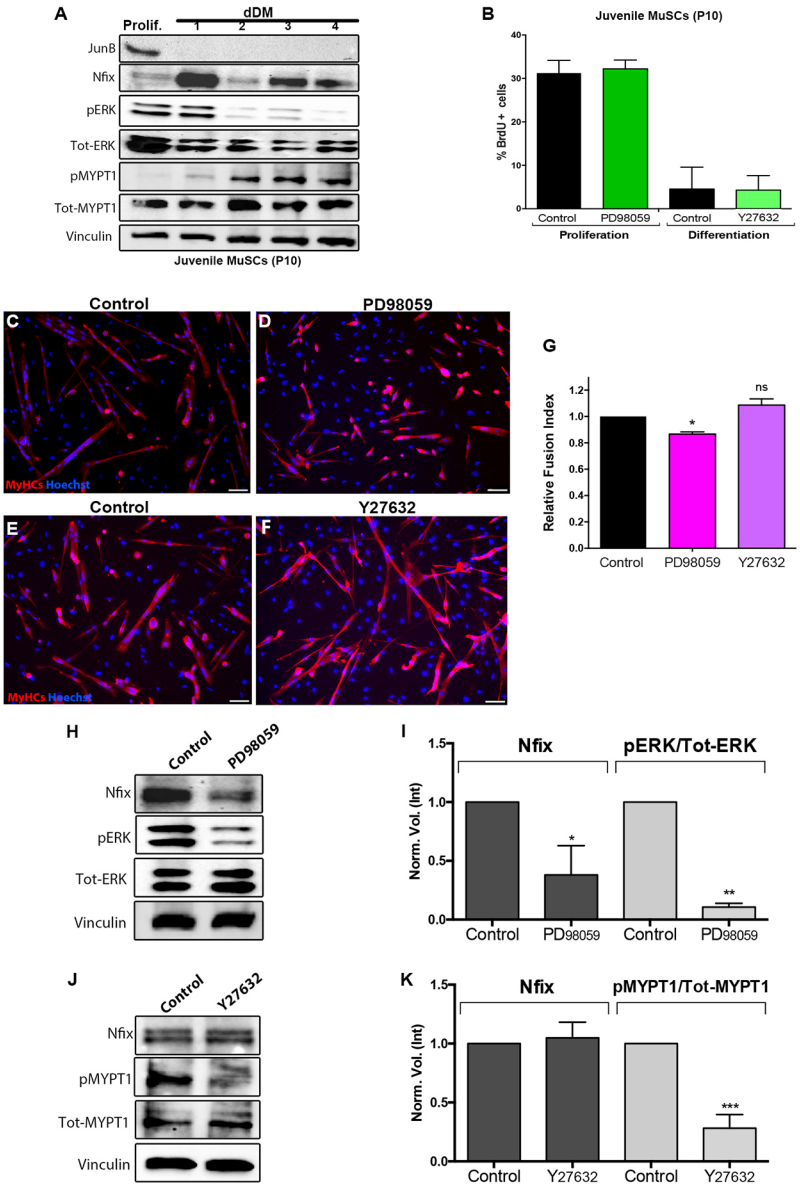

Fig. 7. ERK activity promotes Nfix expression in juvenile MuSCs. (A) Representative western blots of juvenile MuSCs isolated at postnatal day 10 (P10), revealing Nfix, ERK (pERK, totERK) and MyPT1 (pMyPT1, totMyPT1) during proliferation and differentiation (day in differentiation medium, dDM). (B) Quantification of the percentage of proliferative juvenile MuSCs (% BrdU-positive cells) following overnight ERK treatment (proliferation) or 2 days ROCK inhibition, until differentiation (n=5). (C-F) Immunofluorescence of sarcomeric myosins (MyHCs) after PD98059 treatment (C,D) or Y27632 exposure (E,F). The juvenile MuSCs were treated overnight with PD98059 and then allowed to differentiate, whereas the treatment with Y27632 was performed every day until differentiation. Scale bars: 50 µm. (G) Graph of the fusion index relative to control of differentiated satellite cells, treated with PD98059 or Y27632 (*P<0.05; n=5). (H) Western blots of juvenile MuSCs after treatment with the ERK inhibitor PD98059 or vehicle, showing Nfix and ERK (pERK, totERK) during proliferation. (I) Graph showing the densitometric quantification of Nfix and the ratio of pERK on Tot-ERK in juvenile MuSCs treated with PD98059 (*P<0.05; **P<0.01; n=5). (J) Western blots showing Nfix and MyPT1 (pMyPT1, totMyPT1) in juvenile and differentiated MuSCs after daily treatment with the ROCK inhibitor Y27632 or vehicle. Vinculin was used to normalise the amount of loaded protein. (K) Quantification of the densitometry data from western blots of Nfix and the ratio of pMYPT1 on Tot-MYPT1 upon Y27632 treatment in juvenile MuSCs (***P<0.001; n=5).

Development (2018) 145, dev163956. doi:10.1242/dev.163956

control and treated cells for all the analysed myogenic markers. Moreover, we assessed whether the treatments might influence the degree of apoptosis, proliferation and differentiation. As show in Fig. S4I,L, the level of apoptosis through the activation of caspase 3 (aCasp3) and caspase 9 (aCasp9) was not altered by the inhibitors. Treatment with either PD98059 during the proliferative phase or with Y27632 from the start of differentiation (1dDM) did not impinge on the proliferative rate (Fig. 7B), whereas the fusion potential of myogenic cells was reduced after the exposure to PD98059 (Fig. 7C,D,G), as seen for foetal myoblasts. Conversely, the treatment with Y27632 induced only a slight increase in the fusion index of myogenic cells (Fig. 7E-G). Finally, we showed that the inhibition of phosphorylation and activation of the ERK kinases correlated with an impairment of Nfix expression (Fig. 7H,I). In contrast, juvenile MuSCs treated with the ROCK inhibitor during differentiation did not lead to any effects on Nfix expression (Fig. 7J-K, 3dDM).

Taken together, these data suggest that only ERK activity is necessary for the early expression of *Nfix* in juvenile MuSCs, thus confirming that the ERK pathway is conserved from prenatal to postnatal myogenesis. Conversely, the role of RhoA/ROCK in Nfix expression does not appear to be conserved.

DISCUSSION

Nfix plays a crucial role in the transition from embryonic to foetal myogenesis, and thus in the activation of the foetal genetic programme, as well as during muscle regeneration (Messina et al., 2010; Rossi et al., 2016). Therefore, a major objective has been to investigate the mechanism of activation of Nfix with the goal to design pharmacological approaches as a therapeutic strategy for treatment of muscular dystrophies (Rossi et al., 2017a,b). Here, we expose a signalling pathway involving RhoA/ERK/JunB that is crucial for the regulation of Nfix expression.

We initially looked at JunB, as it is the second most expressed transcription factor in foetal myoblasts (Biressi et al., 2007b), and it has been described as an important factor in the physiology of skeletal muscle (Raffaello et al., 2010). We show that JunB and Nfix are co-expressed in foetal progenitor cells, and that JunB modulates Nfix expression, thus defining JunB as an activator of Nfix at the onset of foetal myogenesis. Moreover, these data demonstrate that the foetal genetic programme is fully governed by Nfix, as Nfix expression is essential for the switch between these two phases of prenatal muscle development. We also demonstrate that JunB alone does not regulate this transition from embryonic to foetal myogenesis, although it is necessary for Nfix expression. Of note, a lack of JunB in adult muscle results in atrophic myofibres, owing to the inhibitory effects of JunB on myostatin expression (Raffaello et al., 2010), which represents the same phenotype that we described in the *Nfix*-null mouse (Rossi et al., 2016). Collectively, these observations suggest that JunB may function through its activation of Nfix in adult skeletal muscle. Whether the effect of JunB on Nfix expression is direct or is mediated by other co-factor remains to be investigated.

Given that both JunB and Nfix are necessary for the maintenance of adult skeletal muscle mass, and to further define the signalling involved in the temporal regulation of myogenic progression, we focused on the RhoA GTPases and the ERK kinases. RhoA GTPases and ERK kinases have both been suggested to impact on myofibre size, whereby inhibition of RhoA signalling leads to increased myofibre size (Coque et al., 2014), and inhibition of the ERK cascade leads to muscle atrophy that is associated with reduced myofibre diameters (Haddad and Adams, 2004; Shi et al., 2009). Interestingly, it has also been shown that RhoA activates the Rho kinase ROCK, which in turn inhibits ERK activity (Khatiwala et al., 2009; Li et al., 2013).

Although the relationship between the RhoA and ERK kinase activities had not been characterised in prenatal skeletal muscle development, we speculated that they are involved in the control of JunB and Nfix expression. Indeed, we show increased RhoA and ROCK activities at specific time points throughout embryonic myogenesis, whereas the ERK kinases were activated only during foetal myogenesis. We also demonstrate that the RhoA/ROCK pathway modulates ERK function, the activation of which is essential for promotion of the foetal programme through activation of JunB and Nfix. Therefore, *in vivo* dysfunction of ERK activation during development results in decreased Nfix expression in foetal skeletal muscle. Thus, we show that the RhoA/ROCK-ERK signalling is at least one of the major signalling pathways that regulates the temporal progression of prenatal myogenesis through the promotion of Nfix expression. However, at present, the upstream inputs that orchestrate the modulation of these signalling pathways remain unknown.

In summary, we have defined the RhoA/ROCK pathway as an important regulator of embryonic myogenesis, where it maintains the repression of JunB and Nfix expression through inhibition of ERK activity. However, this role of RhoA/ROCK in the inhibition of Nfix expression is not conserved in juvenile MuSCs. This is not unexpected, as foetal myoblasts and satellite cells are distinct populations of muscle progenitors that differ in terms of their transcriptional expression (Alonso-Martin et al., 2016). Thus, at the onset of foetal myogenesis, RhoA/ROCK signalling progressively decreases, thereby promoting the activation of the ERK kinases, which is in turn necessary for *JunB* and *Nfix* expression. Finally, we demonstrate that the transition from embryonic to foetal muscle is dependent on Nfix, the expression of which is mediated by JunB.

From a biological perspective, our findings represent an important step towards understanding the molecular regulation of *Nfix* expression, and therefore the definition of embryonic and foetal myogenic identities. Moreover, although significant progress has been made in deriving myogenic cells from pluripotent stem cells (Chal et al., 2015; Chal and Pourquié, 2017), methods that can promote robust myogenic differentiation are lacking. Indeed, protocols that allow successful generation of contractile myofibres can only partially reproduce prenatal muscle development, as they do not consider the key step of transition from embryonic to foetal myogenesis. Thus, to generate mature myofibres, in contrast to the thin and short myotubes that are typical of embryonic myofibres, the induction of foetal myogenesis is a prerequisite. The present study might provide a way to overcome the incomplete maturation of differentiated myogenic cells, through manipulation of RhoA/ROCK signalling with Y27632. Fine-tuning of Y27632 concentrations and exposure times will be essential to generate contractile myofibres without introducing exogenous DNA into the cells to force expression of transcription factors.

Finally, a significant translational consequence of the present study is seen from our recent studies on the role of Nfix in muscular dystrophies (Rossi et al., 2017a). Silencing of Nfix in adult skeletal muscle appears to be a promising approach for ameliorating dystrophic phenotypes, and for slowing down the progression of these pathologies. In light of this, the demonstration that Nfix expression is also ERK dependent in postnatal muscle stem cells provides the basis for future therapeutic approaches for muscular dystrophies, for which a medical cure is still needed.

Development (2018) 145, dev163956. doi:10.1242/dev.163956

MATERIALS AND METHODS

Animal work

All mice were kept under pathogen-free conditions with a 12 h/12 h light/dark cycle. All of the procedures on animals conformed to Italian law (D. Lgs n. 2014/26, as the implementation of 2010/63/UE) and were approved by the University of Milan Animal Welfare Body and by the Italian Ministry of Health.

Female mice were mated with males (2:1) and examined every morning for copulatory plugs. The day on which a vaginal plug was seen was designated as gestation day 0.5 (E0.5). All the female mice used for the experiments were at least 7 weeks old. For the *in vivo* evaluation of the effects of PD98059, pregnant mice at day 15.5 of gestation were injected with vehicle (dimethylsulfoxide) or 10 mg/kg PD98059 into the caudal vein.

The following mouse lines were used: *Myf5*$^{GFP\text{-}P/+}$ (Kassar-Duchossoy et al., 2004), *Tg:MLC1f-Nfix2*, *Nfix*-null (obtained from Prof. Richard M. Gronostajski, University of Buffalo, NY, USA) (Campbell et al., 2008) and wild-type CD1 mice (Charles River). The genotyping strategies were as previously published (Kassar-Duchossoy et al., 2004; Messina et al., 2010; Campbell et al., 2008).

Cell isolation and culture

Myf5$^{GFP\text{-}P/+}$ embryonic muscle was isolated at E12.5 and foetal muscles at E16.5. These were mechanically and enzymatically digested for 30 min at 37°C under agitation with 1.5 mg/ml dispase (Gibco), 0.15 mg/ml collagenase (Sigma) and 0.1 mg/ml DNase I (Sigma), as previously described (Biressi et al., 2007b). The dissociated cells were filtered and collected in Dulbecco's modified Eagle's medium (DMEM) with high-glucose (EuroClone), 20% foetal bovine serum (EuroClone), 2 mM EDTA and 20 mM HEPES. The green fluorescent protein (GFP)-positive myoblasts were sorted (BD FACSAria) and cultured in DMEM high-glucose (EuroClone), 20% horse serum (EuroClone), 2 mM L-glutamine (Sigma-Aldrich), 100 IU/ml penicillin and 100 mg/ml streptomycin (Euroclone). The unpurifed embryonic and foetal myoblasts, and the juvenile MuSCs isolated from wild-type postnatal muscle at postnatal day (P) 10, were obtained using the same enzymatic and mechanical procedures used for the Myf5$^{GFP\text{-}P/+}$ myoblasts, and the cells obtained after the digestions were plated onto plastic dishes to allow attachment of the fibroblasts. The non-adherent cells were collected and incubated at 37°C in 20% horse serum in DMEM (EuroClone), in collagen-coated plates. Differentiation was induced by decreasing the horse serum from 20% to 2%. The embryonic myoblasts and juvenile MuSCs were treated daily with 10 µg/ml of the ROCK inhibitor Y27632 (Calbiochem), while the foetal and juvenile MuSCs were treated overnight with 50 µM of the ERK antagonist PD98059 (Cell Signalling). Control cells were treated with vehicle only (dimethylsulfoxide).

Plasmid and lentivirus production

The following plasmids were used: pCH-Nfix2, pCH-HA (Messina et al., 2010); pLentiHA-NfiEngr, pLentiHA-Engr (Messina et al., 2010); scrambled (Sigma-Aldrich) and shJunB plasmids (SHCLNG-NM_008416, Sigma-Aldrich); and PGK-RHOV14, pcDNA3.1X-JunB or pcDNA3.1X as controls. The pcDNA3.1X-JunB plasmid was obtained by subcloning the JunB cDNA (kindly provided by Milena Grossi, Sapienza University of Rome, Italy) into the pcDNA3.1X vector (ThermoFisher). The PGK-RHOV14 plasmid was produced by cloning the cDNA of RhoA with a single point replacement (glycine with valine) at position 14 (RHOV14; kindly provided by Germana Falcone, Consiglio Nazionale delle Ricerche, Rome), in the PGK-GFP vector.

Viral particles were prepared through co-transfection of the packaging plasmids (16.25 µg pMDLg/p; 9 µg pCMV-VSVG; 6.25 µg pRSV-REV) together with each of the following lentiplasmids: shJunB, pLentiHA-Nfix2, PGK-RHOV14 and the respective controls (i.e. scrambled, pLentiHA and PGK). Transfection was performed in HEK293T cells using the calcium phosphate transfection method. The viral particles were collected 40 h after transfection, and concentrated (Lenti-X concentrator; CloneTech), in phosphate-buffered saline (PBS). The concentrated viral particles were stored at -80°C until use.

Cell transfection and transduction

For the transfection experiments, the embryonic or foetal myoblasts were cultured to a confluency of 70% to 80% and transfected following the Lipofectamine LTX (Invitrogen) transfection protocol. The myoblasts were harvested 48 h after transfection. Transduction of foetal myoblasts was performed by addition of the viral preparation to the cultured cells at a multiplicity of infection of 10. After an overnight incubation, the medium was changed and the cells were then maintained in culture for 72 h to allow their differentiation.

Immunofluorescence of cultured cells

Cell cultures were fixed for 10 min at 4°C with 4% paraformaldehyde in PBS, and were then permeabilised with 0.2% Triton X-100 (Sigma-Aldrich), 1% bovine serum albumin (BSA; Sigma-Aldrich) in PBS, for 30 min at room temperature. After permeabilisation, the cells were treated with a blocking solution (10% goat serum; Sigma-Aldrich) for 45 min at room temperature, and then incubated overnight at 4°C with the primary antibodies diluted in PBS. The primary antibodies used were: rabbit anti-Nfix (1:200; Novus Biologicals; NBP2-15039); mouse anti-JunB (1:100; SantaCruz Biotechnology; C-11); mouse anti-total MyHC [hybridoma MF20; 1:2; Developmental Studies Hybridoma Bank (DSHB)]; or rabbit anti-cleaved caspase 3 (1:300; Cell Signalling; D175). After two washes with PBS, 1% BSA and 0.2% Triton, the samples were incubated for 45 min at room temperature with the secondary antibodies (1:250; Jackson Laboratory): goat anti-mouse 594, 92278; goat anti-rabbit 488, 111-545-003) and Hoechst (1:500; Sigma-Aldrich). Finally, the cells were washed twice with 0.2% Triton in PBS and mounted with Fluorescence Mounting Medium (Dako). Images were acquired with a fluorescence microscope (DMI6000B; Leica) equipped with a digital camera (DFC365FX; Leica), and were merged as necessary using Photoshop. Cell counting and evaluation of myotube area were performed using ImageJ. For EdU (5-ethynyl-2′-deoxyuridine) assays, cells were treated for 2 h with 10 µM of EdU solution. After cell fixation and permeabilisation, the detection of EdU was performed following the manufacturer's instructions for the ClickiT Plus EdU Alexa Fluor 647 Imaging Kit (C10640). Conversely, cell cultures were incubated with BrdU (50 µM) in PBS for 1 h at 37°C in 5% CO2 (light off). After two washes with PBS, cells were fixed with 95% ethanol/5% acetic acid 5% for 20 min at room temperature. Then HCl 1.5 M was added for 10 min at room temperature. After two washes with PBS, the cells were permeabilised with 0.25% Triton X-100 (Sigma-Aldrich) for 5 min at room temperature then incubated with the Amersham monoclonal antibody anti-BrdU (GE Healthcare, RPN202) for 1 h at 4°C. After two washes with 1×PBS, 0.25% Triton in PBS was added to cells for 5 min at room temperature. Cells were then incubated with the secondary antibody goat anti-mouse FITC (Alexa Fluor 488 nm, 92589, 1:250, Jackson ImmunoResearch) and Hoechst (1:500; Sigma-Aldrich) for 30 min at room temperature. Finally, the cells were washed twice with PBS and mounted with Fluorescence Mounting Medium (Dako). All the cell counting was performed using ImageJ; statistical analyses were performed with Graphpad.

Immunofluorescence on sections

E16.5 foetuses were fixed overnight with 4% paraformaldehyde solution. After two washes with PBS, the samples were sequentially incubated in PBS supplemented with 7.5%, 15% and 30% of sucrose until completely dehydrated. Foetuses were embed in OCT, frozen in nitrogen-chilled isopentane and kept at −80°C. The sections were prepared at 7 µm and permealised in 1% BSA, 0.2% Triton X-100 in PBS for 30 min at room temperature. The antigens were unmasked by incubating the samples in citrate-based solution [10 mM sodium citrate (pH 6.0) for 20 min at 95-100°C]. The slides were allowed to cool at room temperature and incubated for 1 h with 10% goat serum in PBS. The incubation with primary antibody was performed overnight at 4°C using: rabbit anti-Nfix (1:200, Novus Biologicals; NBP2-15039); mouse anti-total MyHC or anti-Pax7 (hybridoma; 1:2; DSHB); rabbit anti-laminin (1:300, Sigma-Aldrich; L9393). After incubation, the samples were washed and incubated with secondary antibodies (goat anti-mouse 594, 92278; goat anti-rabbit 488, 111-545-003; 1:250, Jackson ImmunoResearch) and Hoechst

Development (2018) 145, dev163956. doi:10.1242/dev.163956

(1:500; Sigma-Aldrich; 861405) for 45 min at room temperature. Finally, the samples were washed in PBS 0.2% Triton X-100 and mounted, and fluorescent immunolabelling was recorded with a DM6000 Leica microscope. Measurement of cross-sectional area (CSA) and cell counting were performed with ImageJ.

RNA extraction, retrotranscripion and real-time qPCR

The extraction of total RNA from cultured cells and from freshly isolated myoblasts was achieved using kits (NucleoSpin RNA XS; Macherey-Nagel). After quantification of the RNA with a photometer (NanoPhotometer; Implen), 0.5 µg total RNA was retrotranscribed (iScript Reverse Transcription Supermix; Bio-Rad). The cDNA obtained was diluted 1:10 in sterile water and 5 µl of the diluted cDNA was used for real-time qPCR. The real-time qPCR was performed using SYBR Green Supermix (Bio-Rad). Relative mRNA expression levels were normalised on GAPDH expression levels. The primers used are listed in Table S1.

Protein extraction and western blotting

Protein extracts were obtained from cultured myoblasts lysed using RIPA buffer [10 mM Tris-HCl (pH 8.0), 1 mM EDTA, 1% Triton-X, 0.1% sodium deoxycholate, 0.1% sodium dodecylsulphate (SDS), 150 mM NaCl, in deionised water] for 30 min on ice, and total protein extracts from embryonic and foetal muscle were obtained from homogenised tissues in tissue extraction buffer (50 mM Tris-HCl, 1 mM EDTA, 1% Triton-X, 150 mM NaCl). Both RIPA and the tissue extraction buffer were supplemented with protease and phosphatase inhibitors. After lysis, the samples were centrifuged at 11,000 ***g*** for 10 min at 4°C, and the supernatants were collected for protein quantification (DC Protein Assays; Bio-Rad).

For western blotting, 30 µg protein of each extract was denaturated at 95°C for 5 min using SDS PAGE sample-loading buffer [100 mM Tris (pH 6.8), 4% SDS, 0.2% bromophenol blue, 20% glycerol, 10 mM dithiothreitol] and loaded onto 8%–12% SDS acrylamide gels. After electrophoresis, the protein was blotted onto nitrocellulose membranes (Protran nitrocellulose transfer membrane; Whatman), which was blocked for 1 h with 5% milk in Tris-buffered saline plus 0.02% Tween20 (Sigma-Aldrich).

The membranes were incubated with the primary antibodies overnight at 4°C under agitation, using the following conditions: rabbit anti-Nfix (1:1000; Novus Biologicals, NBP2-15039), rabbit anti-JunB (1:500; SantaCruz Biotechnology, 210), mouse anti-vinculin (1:2500; Sigma-Aldrich), mouse anti-slow MyHC (hybridoma Bad5; 1:2; DSHB); mouse anti-total MyHC (hybridoma MF20; 1:5; DSHB), rabbit anti-MYPT1 phosphorylated in Thr696 (1:500; SantaCruz Biotechnology, sc-17556-R), rabbit anti-Tot MYPT1 (1:500; SantaCruz Biotechnology, H-130), rabbit anti-pERK (1:1000; SantaCruz Biotechnology, sc-16982-R), mouse anti-Tot ERK (1:500; SantaCruz Biotechnology, sc-135900), mouse anti-Pax7 (hybridoma; 1:5; DSHB), mouse anti-Myogenin (hybridoma; 1:5; DSHB), mouse anti-caspase 9 (1:1000; Cell Signalling Technology, 9508), rabbit anti-caspase 3 (1:1000; Cell Signalling Technology, 9662) and mouse anti-GAPDH (1:5000; Sigma-Aldrich). After incubation with the primary antibodies, the membranes were washed and incubated with the secondary antibodies (1:10,000; IgG-HRP; Bio-Rad) for 40 min at room temperature, and then washed again. The bands were revealed using ECL detection reagent (ThermoFisher), with images acquired using the ChemiDoc MP system (Bio-Rad). The Image Lab software was used to measure and quantify the bands of independent western blot experiments. The obtained absolute quantity was compared with the reference band and expressed in the graphs as normalised volume (Norm. Vol. Int.). All the values are presented as mean±s.d.

Chromatin immunoprecipitation assays

The ChIP protocol was performed on unpurified foetal differentiated myoblasts (E16.5) using 5×10^6 cells for each immunoprecipitation. Foetal myotubes were fixed with 1% formaldehyde (Sigma-Aldrich) in high-glucose DMEM for 10 min at room temperature. The fixation was quenched with 125 mM glycine (Sigma-Aldrich) in PBS for 10 min at room temperature. The cells were rinsed with ice-cold PBS, harvested and centrifuged at 2500 ***g*** for 10 min at 4°C. The cell pellets were lysed and sonicated (Bioruptor sonicator; Diagenode) for 15 min, with repeated cycles of 30 s sonication/30 s rest. The sonicated suspensions were centrifuged at 14,000 ***g*** for 10 min at 4°C, and the supernatants were stored in aliquots at −80°C. Chromatin was precleared with Protein G Sepharose (Amersham) and rabbit serum, for 2 h at 4°C on a rotating platform, and the Protein G Sepharose was blocked overnight with 10 mg/ml BSA and 1 mg/ml salmon sperm (Sigma-Aldrich). After preclearing, the chromantin was incubated overnight at 4°C with 5 µg antibody: rabbit anti-Nfix (Novus Biologicals, NBP2-15039), mouse anti-JunB (SantaCruz Biotechnology, C-11) and normal rabbit IgG (SantaCruz Biotechnology). The following day, the blocked Protein G Sepharose was washed and added to the chromatin incubated with the antibodies, for 3 h under rotation at 4°C. After incubation, the Protein G Sepharose was spun down and repeatedly washed. Elution was performed overnight at 65°C with 10 mg RNase (Sigma-Aldrich) and 200 mM NaCl (Sigma-Aldrich) to reverse the crosslinking. After treatment with 20 µg proteinase K (Sigma-Aldrich), the DNA was purified with phenol/chloroform. The DNA obtained was analysed using real-time qPCR, and the data were plotted as fold-enrichment with respect to the IgG sample. The primers used are listed in Table S1.

Pull-down assays

Active Rho Pull-Down and Detection kits (ThermoScientific) were used with 600 µg cell lysate obtained from unpurified myoblasts (E12.5, E14.5 and E16.5) following the manufacturer instructions.

Statistical analysis

Graphs were constructed and Student's *t*-tests performed using GraphPad Prism 6.0e. The statistics are reported in the text as mean±s.d. (n=5). CSA distribution is expressed as mean±whiskers from minimum to maximum. Statistical significance was analysed using an unpaired two-tailed Student's *t*-tests (homoscedastic): *P<0.1; **P<0.05; ***P<0.01.

Acknowledgements

We thank M. Grossi for the JunB plasmid, and G. Maroli, G. Cossu and G. Rossi for helpful discussions. We are also grateful to R. Gronostajski for the kind exchange of information and animal models.

Competing interests

The authors declare no competing or financial interests.

Author contributions

Conceptualization: V.T., G. Messina; Methodology: V.T., G.A., G. Mura, C.B., E.C., S.M., G.L.C.; Validation: G.A., G. Mura., V.T.; Formal analysis: V.T.; Investigation: V.T., G.A., G. Mura, C.B., E.C., S.M.; Resources: G. Messina; Data curation: V.T.; Writing - original draft: V.T.; Writing - review & editing: S.T., F.R., G. Messina; Supervision: G. Messina; Project administration: G. Messina; Funding acquisition: G. Messina.

Funding

This study was funded by the European Research Council, ERC StG2011 (RegeneratioNfix 280611). F.R. acknowledges support from the Association Française contre les Myopathies via TRANSLAMUSCLE (project 19507). S.T. acknowledges support from the Institut Pasteur and the Agence Nationale de la Recherche (Laboratoire d'Excellence Revive, ANR-10-LABX-73).

Supplementary information

Supplementary information available online at
http://dev.biologists.org/lookup/doi/10.1242/dev.163956.supplemental

References

Alonso-Martin, S., Rochat, A., Mademtzoglou, D., Morais, J., de Reyniès, A., Auradè, F., Chang, T. H.-T., Zammit, P. S. and Relaix, F. (2016). Gene expression profiling of muscle stem cells identifies novel regulators of postnatal myogenesis. *Front. Cell. Dev. Biol.* **4**, 58.

Amano, M., Ito, M., Kimura, K., Fukata, Y., Chihara, K., Nakano, T., Matsuura, Y. and Kaibuchi, K. (1996). Phosphorylation and activation of myosin by Rho-associated kinase (Rho-kinase). *J. Biol. Chem.* **271**, 20246-20249.

An, C.-I., Dong, Y. and Hagiwara, N. (2011). Genome-wide mapping of Sox6 binding sites in skeletal muscle reveals both direct and indirect regulation of muscle terminal differentiation by Sox6. *BMC Dev. Biol.* **11**, 59.

Bachurski, C. J., Yang, G. H., Currier, T. A., Gronostajski, R. M. and Hong, D. (2003). Nuclear factor I/thyroid transcription factor 1 interactions modulate surfactant protein C transcription. *Mol. Cell. Biol.* **23**, 9014-9024.
Biressi, S., Molinaro, M. and Cossu, G. (2007a). Cellular heterogeneity during vertebrate skeletal muscle development. *Dev. Biol.* **308**, 281-293.
Biressi, S., Tagliafico, E., Lamorte, G., Monteverde, S., Tenedini, E., Roncaglia, E., Ferrari, S., Ferrari, S., Cusella-De Angelis, M. G., Tajbakhsh, S. et al. (2007b). Intrinsic phenotypic diversity of embryonic and fetal myoblasts is revealed by genome-wide gene expression analysis on purified cells. *Dev. Biol.* **304**, 633-651.
Campbell, C. E., Piper, M., Plachez, C., Yeh, Y.-T., Baizer, J. S., Osinski, J. M., Litwack, E. D., Richards, L. J. and Gronostajski, R. M. (2008). The transcription factor Nfix is essential for normal brain development. *BMC Dev. Biol.* **8**, 52.
Castellani, L., Salvati, E., Alemà, S. and Falcone, G. (2006). Fine regulation of RhoA and Rock is required for skeletal muscle differentiation. *J. Biol. Chem.* **281**, 15249-15257.
Chal, J. and Pourquié, O. (2017). Making muscle: skeletal myogenesis in vivo and in vitro. *Development* **144**, 2104-2122.
Chal, J., Oginuma, M., Al Tanoury, Z., Gobert, B., Sumara, O., Hick, A., Bousson, F., Zidouni, Y., Mursch, C., Moncuquet, P. et al. (2015). Differentiation of pluripotent stem cells to muscle fiber to model Duchenne muscular dystrophy. *Nat. Biotechnol.* **33**, 962-969.
Chapman, V. M., Miller, D. R., Armstrong, D. and Caskey, C. T. (1989). Recovery of induced mutations for X chromosome-linked muscular dystrophy in mice. *Proc. Natl. Acad. Sci. USA* **86**, 1292-1296.
Chinenov, Y. and Kerppola, T. K. (2001). Close encounters of many kinds: Fos-Jun interactions that mediate transcription regulatory specificity. *Oncogene* **20**, 2438-2452.
Coque, E., Raoul, C. and Bowerman, M. (2014). ROCK inhibition as a therapy for spinal muscular atrophy: understanding the repercussions on multiple cellular targets. *Front. Neurosci.* **8**, 271.
Duclos, F., Straub, V., Moore, S. A., Venzke, D. P., Hrstka, R. F., Crosbie, R. H., Durbeej, M., Lebakken, C. S., Ettinger, A. J., van der Meulen, J. et al. (1998). Progressive muscular dystrophy in alpha-sarcoglycan-deficient mice. *J. Cell Biol.* **142**, 1461-1471.
Eferl, R. and Wagner, E. F. (2003). AP-1: a double-edged sword in tumorigenesis. *Nat. Rev. Cancer* **3**, 859-868.
Gronostajski, R. M. (2000). Roles of the NFI/CTF gene family in transcription and development. *Gene* **249**, 31-45.
Haddad, F. and Adams, G. R. (2004). Inhibition of MAP/ERK kinase prevents IGF-I-induced hypertrophy in rat muscles. *J. Appl. Physiol.* **96**, 203-210.
Hutcheson, D. A., Zhao, J., Merrell, A., Haldar, M. and Kardon, G. (2009). Embryonic and fetal limb myogenic cells are derived from developmentally distinct progenitors and have different requirements for beta-catenin. *Genes Dev.* **23**, 997-1013.
Jiang, P., Song, J., Gu, G., Slonimsky, E., Li, E. and Rosenthal, N. (2002). Targeted deletion of the MLC1f/3f downstream enhancer results in precocious MLC expression and mesoderm ablation. *Dev. Biol.* **243**, 281-293.
Kassar-Duchossoy, L., Gayraud-Morel, B., Gomès, D., Rocancourt, D., Buckingham, M., Shinin, V. and Tajbakhsh, S. (2004). Mrf4 determines skeletal muscle identity in Myf5:Myod double-mutant mice. *Nature* **431**, 466-471.
Khatiwala, C. B., Kim, P. D., Peyton, S. R. and Putnam, A. J. (2009). ECM compliance regulates osteogenesis by influencing MAPK signaling downstream of RhoA and ROCK. *J. Bone Miner. Res.* **24**, 886-898.
Kimura, K., Ito, M., Amano, M., Chihara, K., Fukata, Y., Nakafuku, M., Yamamori, B., Feng, J., Nakano, T., Okawa, K. et al. (1996). Regulation of myosin phosphatase by Rho and Rho-associated kinase (Rho-kinase). *Science* **273**, 245-248.
Li, F., Jiang, Q., Shi, K. J., Luo, H., Yang, Y. and Xu, C. M. (2013). RhoA modulates functional and physical interaction between ROCK1 and Erk1/2 in selenite-induced apoptosis of leukaemia cells. *Cell Death Dis.* **4**, e708.
Mathew, S. J., Hansen, J. M., Merrell, A. J., Murphy, M. M., Lawson, J. A., Hutcheson, D. A., Hansen, M. S., Angus-Hill, M. and Kardon, G. (2011). Connective tissue fibroblasts and Tcf4 regulate myogenesis. *Development* **138**, 371-384.
Messina, G., Biressi, S., Monteverde, S., Magli, A., Cassano, M., Perani, L., Roncaglia, E., Tagliafico, E., Starnes, L., Campbell, C. E. et al. (2010). Nfix regulates fetal-specific transcription in developing skeletal muscle. *Cell* **140**, 554-566.
Mourikis, P., Gopalakrishnan, S., Sambasivan, R. and Tajbakhsh, S. (2012). Cell-autonomous Notch activity maintains the temporal specification potential of skeletal muscle stem cells. *Development* **139**, 4536-4548.
Murányi, A., Derkach, D., Erdődi, F., Kiss, A., Ito, M. and Hartshorne, D. J. (2005). Phosphorylation of Thr695 and Thr850 on the myosin phosphatase target subunit: inhibitory effects and occurrence in A7r5 cells. *FEBS Lett.* **579**, 6611-6615.
Nishiyama, T., Kii, I. and Kudo, A. (2004). Inactivation of Rho/ROCK signaling is crucial for the nuclear accumulation of FKHR and myoblast fusion. *J. Biol. Chem.* **279**, 47311-47319.
Pelosi, M., Marampon, F., Zani, B. M., Prudente, S., Perlas, E., Caputo, V., Cianetti, L., Berno, V., Narumiya, S., Kang, S. W. et al. (2007). ROCK2 and its alternatively spliced isoform ROCK2m positively control the maturation of the myogenic program. *Mol. Cell. Biol.* **27**, 6163-6176.
Pistocchi, A., Gaudenzi, G., Foglia, E., Monteverde, S., Moreno-Fortuny, A., Pianca, A., Cossu, G., Cotelli, F. and Messina, G. (2013). Conserved and divergent functions of Nfix in skeletal muscle development during vertebrate evolution. *Development* **140**, 1528-1536.
Raffaello, A., Milan, G., Masiero, E., Carnio, S., Lee, D., Lanfranchi, G., Goldberg, A. L. and Sandri, M. (2010). JunB transcription factor maintains skeletal muscle mass and promotes hypertrophy. *J. Cell Biol.* **191**, 101-113.
Rossi, G., Antonini, S., Bonfanti, C., Monteverde, S., Vezzali, C., Tajbakhsh, S., Cossu, G. and Messina, G. (2016). Nfix regulates temporal progression of muscle regeneration through modulation of myostatin expression. *Cell Rep.* **14**, 2238-2249.
Rossi, G., Bonfanti, C., Antonini, S., Bastoni, M., Monteverde, S., Innocenzi, A., Saclier, M., Taglietti, V. and Messina, G. (2017a). Silencing Nfix rescues muscular dystrophy by delaying muscle regeneration. *Nat. Commun.* **8**, 1055.
Rossi, G., Taglietti, V. and Messina, G. (2017b). Targeting Nfix to fix muscular dystrophies. *Cell Stress* **2**, 17-19.
Schiaffino, S. and Reggiani, C. (2011). Fiber types in mammalian skeletal muscles. *Physiol. Rev.* **91**, 1447-1531.
Seko, T., Ito, M., Kureishi, Y., Okamoto, R., Moriki, N., Onishi, K., Isaka, N., Hartshorne, D. J. and Nakano, T. (2003). Activation of RhoA and inhibition of myosin phosphatase as important components in hypertension in vascular smooth muscle. *Circ. Res.* **92**, 411-418.
Shi, H., Scheffler, J. M., Zeng, C., Pleitner, J. M., Hannon, K. M., Grant, A. L. and Gerrard, D. E. (2009). Mitogen-activated protein kinase signaling is necessary for the maintenance of skeletal muscle mass. *Am. J. Physiol. Cell Physiol.* **296**, C1040-C1048.
Taglietti, V., Maroli, G., Cermenati, S., Monteverde, S., Ferrante, A., Rossi, G., Cossu, G., Beltrame, M. and Messina, G. (2016). Nfix induces a switch in Sox6 transcriptional activity to regulate MyHC-I expression in fetal muscle. *Cell Rep* **17**, 2354-2366.
Uehata, M., Ishizaki, T., Satoh, H., Ono, T., Kawahara, T., Morishita, T., Tamakawa, H., Yamagami, K., Inui, J., Maekawa, M. et al. (1997). Calcium sensitization of smooth muscle mediated by a Rho-associated protein kinase in hypertension. *Nature* **389**, 990-994.
Zuckerbraun, B. S., Shapiro, R. A., Billiar, T. R. and Tzeng, E. (2003). RhoA influences the nuclear localization of extracellular signal-regulated kinases to modulate p21Waf/Cip1 expression. *Circulation* **108**, 876-881.